# Physical Properties of Nanostructured Fese Thin Films Deposited by Chemical Bath Deposition Techniques: Effect of Fe(NO3)3.9H2O Source

Yogesh S. Sakhare, Monali V. Bhute, Milind R. Belkhedkar, S. G. Ibrahim, Ashok U. Ubale*

Nanostructured Thin Film Materials Laboratory, Department of Physics, Govt. Vidarbha Institute of Science and Humanities, Amravati 444 604, India

## ABSTRACT

The simple, economic and convenient chemical bath deposition technique is utilized to grow nanostructured FeSe thin films at room temperature. The effect of Fe ion source, Fe (NO3)3.9H2O on growth process of FeSe thin films is discussed. The X-ray diffraction study revealed that the CBD deposited FeSe thin films are polycrystalline in nature with hexagonal type lattice. The morphological investigations carried from SEM and AFM analysis shows that FeSe grains are uniformly distributed over the entire substrate surface. The electrical resistivity of FeSe films is of the order of $104\Omega$-cm. The thermo-emf measurements confirms its P-type conductivity.

## KEYWORDS

FeSe, thin films, Optical and Electrical properties

## 1. INTRODUCTION

The nanostructured chalcogenide thin films have been extensively studied both theoretically and experimentally to get novel structural optical and electrical properties, suitable for technological development. They play a vital role in integrated circuits and various optoelectronic devices, which in general are made of one or more functional layers with pertinent characteristics. For example, a thin film solar cell consists of an absorber layer, a buffer layer and a window layer in addition to the metal layers, which provide ohmic contact to the cell. Selenium based chalcogenides have extensive applications in electronic and optoelectronic devices [1], due to their transparency in IR region, good thermal, mechanical and chemical properties [2]. Selenium is a promising material for large number of applications in xerography, photocells, switching and memory devices. In the last decade many metal selenide thin films have been extensively studied, but there is no systematic study regarding growth of FeSe thin films by chemical bath at low temperature. The Fe-Se compounds, such as FeSe, FeSe2, Fe3Se4 and Fe7Se8 etc [3-6] are important phases of Se based materials.

The iron chalcogenide compounds have attracted much attention of research community due to its potential application as an absorber in solar cells [7–12]. Various techniques have been used for the synthesis of FeSe thin films; such as sputtering, electrodeposition, vacuum evaporation, screen printing, photochemical deposition and spray pyrolysis [13-15]. The aim of the present study is to deposit FeSe thin films on glass substrates by chemical bath deposition technique and investigate the effect of Fe ion source on growth process as well as on structural morphological properties.

## 2. EXPERIMENTAL

Thin films of iron selenide were grown by using slow release of Fe2+ ions from EDTA complexed Fe salt and Se2- ions in aqueous medium using CBD method. The analytical grade reagents Fe(NO3)3.9H2O, EDTA and Se metals powder and sodium sulfide were used in the present work. The commercially available glass micro slides of dimensions 26 mm×76 mm×2 mm were boiled in chromic acid for 30 min and were washed with double distilled water. The substrates were than washed with liquid detergent and rinsed in acetone. Finally slides were ultrasonically cleaned for 15 min in double distilled water prior to the actual deposition. For the deposition of FeSe thin films 40 ml of 0.03 M, Fe (NO3)3.9H2O is mixed with 20 ml of 0.1M, EDTA and 40 ml of freshly prepared 0.13 M, Na2SeSO3. The uniform and well adherent secularly reflecting orange brown coloured thin films were removed after 72 h deposition time from the bath and washed with distilled water. In order to investigate deposition mechanism and the effect of molar concentration of Fe (NO3)3.9H2O on growth process and its impact on the structural, and morphological properties different sets of FeSe films were prepared by changing its molar concentration from 0.03 to 0.18 M.

The X-ray diffraction (XRD) studies were carried by using PANalytical X'Pert PRO MRD X-ray diffractometer with Cukα radiation in the two theta range from 20 to 90 degree. The scanning electron micrographs (SEM) and energy-dispersive X-ray spectroscopy (EDS) were acquired from a JOEL'S JSM-7600F microscope having resolution of 1 nm. Using Park Scientific Instruments, the two and three dimensional AFM images of FeSe are studied to analyze surface morphology. The two-point dc probe method of dark electrical resistivity was used to study the electrical resistivity. The thermo-emf measurements of FeSe films were carried by applying temperature gradient across the sample to find the type of conductivity.

## 3. RESULTS AND DISCUSSION

The deposition of FeSe thin film occurs when the ionic product of Fe2+ and Se2− ions exceeds the solubility product of FeSe. The controlled release of Fe2+ and Se2− ions in the solution controls the rate of precipitation and hence the rate of film formation. The steps involved in the chemical deposition of FeSe thin films are given below.

The hydrolysis of sodium selenosulphate (Na2SeSO3) takes place to give Se2− ions as,

$$Na_2SeSO_3 + OH^- \rightarrow Na_2SO_4 + HSe^- \qquad (1)$$

$$HSe^- + OH^- \rightarrow H_2O + Se^{2-} \qquad (2)$$
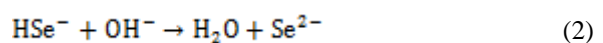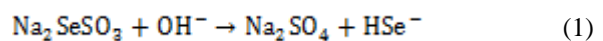
The metal ions from $Fe(NO_3)_3.9H_2O$ forms complex with EDTA as,

$$Fe(NO_3)_3 . 9H_2O + EDTA_{(aq)} \rightarrow [FeEDTA]^{2+} + (NO_3)^-$$

(3)
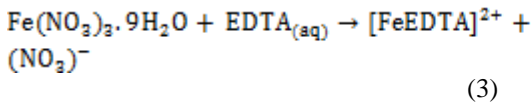
The complex decomposition takes place to release $Fe^{2+}$ ions,

$$[FeEDTA]^{2+} \rightarrow Fe^{2+} + EDTA_{(aq)}$$

(4)
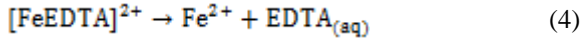
Finally, FeSe thin film formation takes place as,

$$Fe^{2+} + Se^{2-} \rightarrow FeSe \downarrow$$

(5)

Figure 1 shows the variation of FeSe film thickness with molar concentration of Fe source. It was observed that at lower molar concentration very few number of Fe2+ ions are available for the formation of FeSe solid phase. Below this concentration no film formation is observed, it may because the ionic product of Fe2+ and Se2- is less than solubility product of FeSe. The film thickness linearly increases with concentration up to 0.12 M and then the growth rate is slowly decreased. It may be because after 0.12 M concentration the ion-by-ion growth mechanism is suppressed by cluster-by-cluster deposition giving powdery film.

The peaks observed at 28.401 and 48.131 corresponds to the (100) and (110) orientations due to hexagonal phase (Fig.2). However, the (230) orientation is observed due to FeSe2 at lower thickness. At lower molar concentration the numbers of Fe2+ ions available to from FeSe phase are less as compare to Se2- ions. The crystallite size was determined from (100) diffraction peak using the Scherrer formula [13],

$$d = \frac{0.9\lambda}{\beta Cos\theta}$$

(6)

Where $\lambda$ is the wavelength used (0.154 nm); $\beta$ is the angular line width at half maximum intensity in radians; $\theta$ is the Bragg's angle. The grain size at 0.03 molar concentration is 45 nm and it increases to 81 nm at 0.12 molar concentrations and then again decreases for further rise in concentration. The crystallite size has thus shown dependence on deposition mechanism, the cluster-by-cluster mechanism at higher concentration gives smaller grains than the ion-by-ion mechanism at lower concentration.
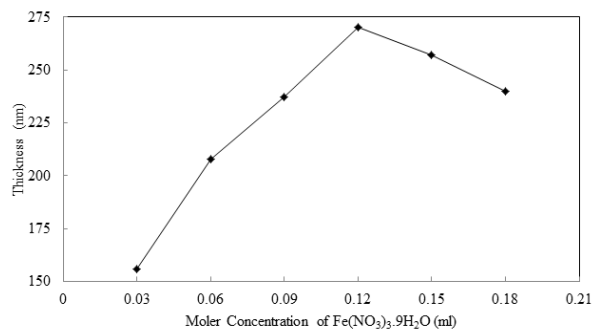


**Fig.1. Variation of FeSe film thickness (nm) with molar concentration of Fe (NO₃)₃·9H₂O.**
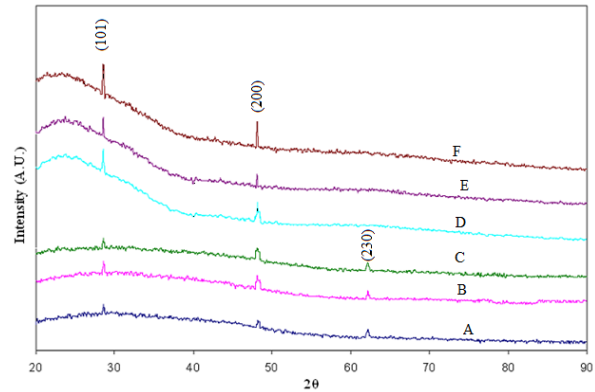


**Fig.2. X-ray diffraction pattern of FeSe thin films deposited at various molar concentrations of $Fe(NO_3)_3.9H_2O$: (A) 0.03M ,(B) 0.06M , (C) 0.09M , (D) 0.12M ,(E) 0.15M and (F) 0.18M.**

The surface morphology of FeSe thin films deposited using different molar concentration of Fe2+ was examined by scanning electron microscopy (SEM) and presented in fig(3). The surface morphology is found to be dependent on deposition mechanism. At lower concentration of Fe source, as the deposition rate is very small (ion-by-ion growth), the film surface is uniformly covered and it increases linearly with molar concentration. After 0.09 molar concentration the film surface shows overgrowth and becomes slightly porous. Growth of some nano-rods and nano-plates are also observed at higher thickness. The films surface after 0.12 M concentration becomes slightly powdery, accordingly the SEM images also shows agglomeration of grains on the surface.
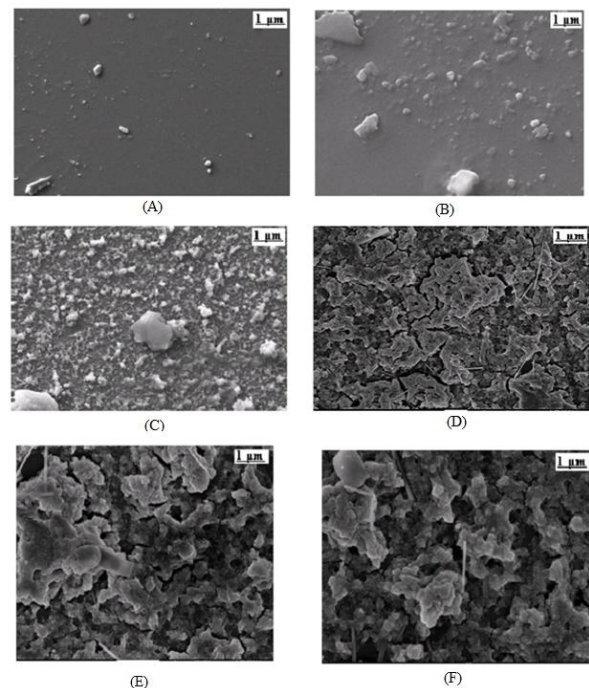


**Fig.3. SEM images of FeSe thin films deposited at various molar concentrations of Fe(NO3)3.9H2O: (A) 0.03M ,(B) 0.06M , (C) 0.09M , (D) 0.12M ,(E) 0.15M and (F) 0.18M.**

Two and three-dimensional surface morphology of the chemically deposited FeSe thin film was investigated by taking AFM images. Fig. 4 shows the 3D and 2D AFM images of FeSe film deposited from 0.03 and 012 M concentration of Fe source. From the micrographs, one can see the total coverage of the substrate with uniform growth of spherical grains. The RMS roughness of film surface is 69 to 105 nm for the films of thickness 156 and 270nm. The film surface at lower thickness is almost smooth and independent of the scanning area chosen.

Fig.5 shows the variation of room temperature electrical resistivity of FeSe with molar concentration of Fe(NO3)3.9H20. The electrical resistivity of FeSe is $59 \times 10^4$ $\Omega$-cm at lower thickness i.e. at 0.13 M concentration of Fe source and it decreases to $11 \times 10^4$ $\Omega$-cm as molar concentration of Fe source is increased to 0.12 M, which may be due to improvement in film thickness and crystalline quality of FeSe. The improvement in crystalline nature with thickness enhances the concentration and mobility of Fe ion vacancies within the lattice and hence reduces the resistivity of the films
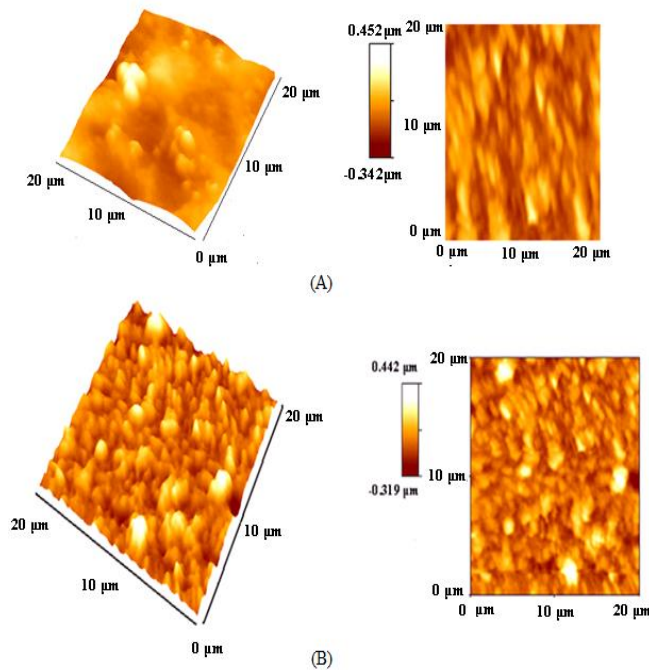


**Fig.4. 2D and 3D-AFM images of FeSe thin films deposited at (A) 0.03 M and (B)0.12 M molar concentration of Fe(NO3)3.9H2O .**

The temperature difference applied across a semiconducting film causes a transport of carriers from the hot to cold end and thus creates an electric field, called thermo-emf. From the thermo-emf measurements, one can determine whether the electrons or holes make the dominant contribution to the conduction mechanism. The temperature of the cold end was maintained at 273 K using cold water and the hot end was heated using strip type heaters. The thermo-emf measurements showed that the FeSe thin films have p-type electrical conductivity which may be due to the presence of Fe ion vacancies within the lattice. The p-type electrical conductivity of FeSe is in good agreement with the literature [16].The thermo-emf increases linearly with applied temperature difference [fig 6]. The increase in thermo-emf with temperature can be attributed to the increase in carrier concentration and/or mobility of the charge carriers.
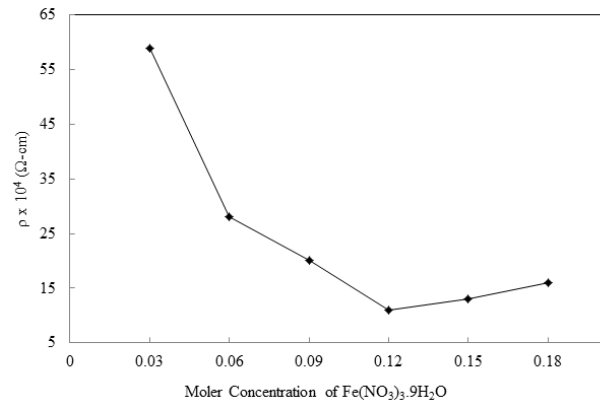


**Fig.5.Variation of electrical resistivity ($\Omega$-cm) of FeSe at 373 K temperature with molar concentration of Fe(NO3)3.9H2O.**
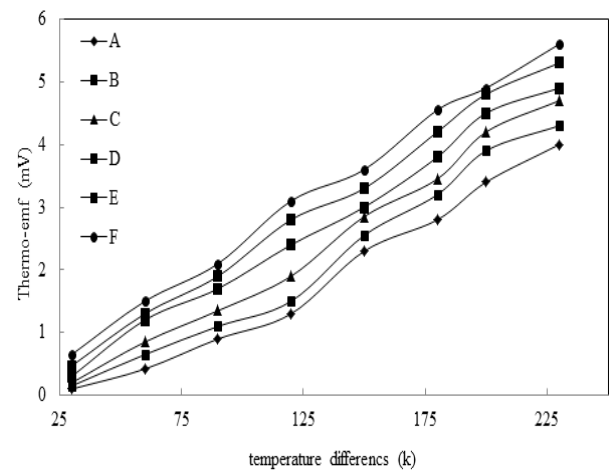


**Fig.6. Variation of thermo-e.m.f. (mV) versus temperature differences across the FeSe thin film deposited at various moler concentrations of Fe(NO3)3.9H2O : (A) 0.03M ,(B) 0.06M , (C) 0.09M , (D) 0.12M ,(E) 0.15M and (F) 0.18M.**

## 4. CONCLUSITIONS

The FeSe thin films were deposited using CBD method on to glass substrates by changing molar concentration of Fe(NO3)3.9H20 0.03 from to 018 M. The electrical resistivity confirms semiconducting nature and the room temperature resistivity is of the order of $59 \times 10^4$ $\Omega$-cm for as prepared FeSe film, which decreased to $13 \times 10^4 \Omega$-cm as the molar concentration of Fe (NO3)3.9H2O solution changes from 0.03 to 0.12 M. The thermo-emf measurements confirm P-type conductivity of FeSe. The XRD study shows hexagonal crystal structure. The SEM and AFM studies show porous morphology. The thin films deposited at 0.12 Molar concentration of Fe(N03)3.9H20 are found more suitable for application purpose.

## ACKNOWLEDGEMENT

## 5. REFERENCES

[1] J.M. Harbold, F. O. Wise and B.G. Itkain, IEEE Photonics Technilogy Letters,14 (2002) 822.

[2] Y. Nedeva, T. Petkova, E. Mytillneou, P.Petkov, J.of Optoele.s & Adv.mater.,3 (2001) 433.

[3] H. Tokutaro, M. Seijiro, T. Noboru, J. Phys. Soc. Jpn. 9 (1954) 496.

[4] H. Kinshiro, J. Phys. Soc. Jpn. 12 (1957) 929.

[5] E.C. Kim, S.G. Kang, I.H. Cho, Y.S. Hwang, H.G. Hwang, J.G. Kim,J. Appl. Phys. 81 (1997) 4131.

[6] C.E.M. Campos, J.C. de Lima, T.A. Grandi, K.D. Machado, V. Drago, P.S.Pizani, J. Magn. Magn.Mater. 270 (2004) 89.

[7] A. Ennaoui, S. Fiechter, Ch. Pettenkofer, N. Alonoso-Vante, K. Buker, M. Bronold, Ch. Hopfner, H. Tribudou, Sol. Energy Mater. Sol. Cells 29 (1993) 289.

[8] N. Hamdadou, A. Khelil, J.C. Bernede, Mater. Chem. Phys. 78 (2003) 591.

[9] A. Ennaoui, H. Tributch, Sol. Energy Mater. 14 (1986) 461.

[10] V. Antonucci, A.S. Arico, N. Giordano, P.L. Antonucci, U. Russo, D.L. Cocke, F. Crea, Sol. Cells 31 (1991) 31.

[11] A.S. Arico, V. Antonucci, P.L. Antonucci, D.L. Cocke, U. Russo, N. Giordano, Sol. Energy Mater. 20 (1990) 323.

[12] A.S. Arico, V. Antonucci, N. Giordano, F. Crea, P.L. Antonucci, Mater. Chem. Phys. 28 (1991) 75.

[13] Y. Takemura, H. Suto, N. Honda, K. Kakuno, K. Saito, J. Appl. Phys. 81 (1997) 5177.

[14] C.E.M. Campos, J.L. de lima, T.A. Grandi, K.D. Machado, P.S. Pizami, Solid State Commun. 23 (2003) 179.

[15] B. Ouertani, J. Ouertfelli, M. Saadoun, B. Bessais, M. Hajji, M. Kanzari, H. Ezzaouia, N. Hamdadou, Mater. Lett. 59 (2005) 734.

[16] S.M. Pawar, A.V. Moholkar, U.B. Suryavanshi, K.Y. Rajpure, C.H. Bhosale, Sol. Energy Mater. Sol. Cells 91 (2007) 560.